

Optimal location of thalamotomy lesions for tremor associated with Parkinson disease: a probabilistic analysis based on postoperative magnetic resonance imaging and an integrated digital atlas

JEFFREY D. ATKINSON, M.D., D. LOUIS COLLINS, PH.D.,
GILLES BERTRAND, O.C., M.D., M.Sc., F.R.C.S.(C), TERRY M. PETERS, PH.D., F.C.C.P.M.,
G. BRUCE PIKE, PH.D., AND ABBAS F. SADIKOT, M.D., PH.D., F.R.C.S.(C)

Division of Neurosurgery, McConnell Brain Imaging Center, Montreal Neurological Institute, McGill University, Montreal, Quebec; and Imaging Research Labs, The John P. Robarts Research Institute, London, Ontario, Canada

Object. Renewed interest in stereotactic neurosurgery for movement disorders has led to numerous reports of clinical outcomes associated with different treatment strategies. Nevertheless, there is a paucity of autopsy and imaging data that can be used to describe the optimal size and location of lesions or the location of implantable stimulators. In this study the authors correlated the clinical efficacy of stereotactic thalamotomy for tremor with precise anatomical localization by using postoperative magnetic resonance (MR) imaging and an integrated deformable digital atlas of subcortical structures.

Methods. Thirty-one lesions were created by stereotactic thalamotomy in 25 patients with tremor-dominant Parkinson disease. Lesion volume and configuration were evaluated by reviewing early postoperative MR images and were correlated with excellent, good, or fair tremor outcome categories. To allow valid comparisons of configurations of lesions with respect to cytoarchitectonic thalamic boundaries, the MR image obtained in each patient was nonlinearly deformed into a standardized MR imaging space, which included an integrated atlas of the basal ganglia and thalamus. The volume and precise location of lesions associated with different clinical outcomes were compared using nonparametric statistical methods. Probabilistic maps of lesions in each tremor outcome category were generated and compared.

Statistically significant differences in lesion location between excellent and good, and excellent and fair outcome categories were demonstrated. On average, lesions associated with excellent outcomes involved thalamic areas located more posteriorly than sites affected by lesions in the other two outcome groups. Subtraction analysis revealed that lesions correlated with excellent outcomes necessarily involved the interface of the nucleus ventralis intermedialis (Vim; also known as the ventral lateral posterior nucleus [VLp]) and the nucleus ventrocaudalis (Vc; also known as the ventral posterior [VP] nucleus). Differences in lesion volume among outcome groups did not achieve statistical significance.

Conclusions. Anatomical evaluation of lesions within a standardized MR image-atlas integrated reference space is a useful method for determining optimal lesion localization. The results of an analysis of probabilistic maps indicates that optimal relief of tremor is associated with lesions involving the Vim (VLp) and the anterior Vc (VP).

KEY WORDS • thalamus • atlas • Parkinson disease • tremor • magnetic resonance imaging

IMPROVED knowledge of basal ganglia pathophysiology and availability of modern imaging procedures has resulted in a renewed interest in surgery for movement disorders.^{32,94} Preferences for different surgical targets have continued to evolve,^{6,16,61–63,86,94} and a more rational treat-

ment approach should emerge as more clinical outcome data for the various procedures become available. In the case of stereotactic lesioning methods, the size and configuration of the lesion may be as relevant to clinical outcome as the choice of the target itself. Therefore, valid comparisons of clinical outcomes of different stereotactic strategies require correlation with precise target localization. In addition, specific information about morphological changes induced by the surgical procedure may be helpful in elucidating the mechanism of therapeutic effects and in improving our understanding of brain function in healthy and pathological states. Although numerous studies have provided information on clinical results, there are few systematic reports in which clinical effectiveness has been correlated with lesion size and location.^{7,18,22,37,41,43,44,60,66,67,72,84,89}

Detailed examination of the accuracy and precision of stereotactic procedures is limited because, at the micro-

Abbreviations used in this paper: AC = anterior commissure; CT = computerized tomography; MR = magnetic resonance; PC = posterior commissure; PD = Parkinson disease; SD = standard deviation; SEM = standard error of the mean; 3D = three-dimensional. Thalamic nuclei: CM = centromedian; Dim = dorsointermedialis; Vc = ventrocaudalis; Vcae = Vc anterior externus; Vcai = Vc anterior internus; Vce = Vc externus; Vci = Vc internus; Vim = ventralis intermedialis; VLa = ventral lateral anterior; VLp = ventral lateral posterior; Voa = ventrooralis anterior; Voi = ventrooralis internus; Vop = ventrooralis posterior; VP = ventral posterior; VPL = ventral posterior lateral; VPLa = anterior division of the VPL; VPM = ventral posterior medial; Zc = zentrolateralis caudalis.

Thalamotomy lesion evaluation

scopic level, anatomy cannot be examined in the living human brain. A relatively small number of autopsy series^{7,41,44,47,72} have provided descriptions of the volume and position of lesions. Although imaging studies do not currently provide the level of spatial detail available in histological studies, improved characterization of stereotactic lesions may be obtained using CT⁴³ or MR imaging.^{18,37,84,102,104} Note that although MR images are superior in quality to CT scans, most MR imaging systems in routine use have significant limitations in spatial resolution and structural differentiation. Detailed examination of anatomical cytoarchitectonic boundaries of subcortical nuclei is not possible within the current clinical imaging environment.

Digitized or computerized atlases may be used to increase the degree of structural detail on clinical imaging studies. A digitized atlas may be integrated with MR images or CT scans by selecting landmarks or boundaries visible on the image and outlined in the atlas and by using mathematical transformations to scale the atlas to fit the specific image. Scaled digitized atlases matched to a CT or MR image can enhance the planning of stereotactic procedures,^{3,58,76,83,93} and linear scaling has the advantage of relatively rapid integration. Nonlinear deformation would allow for a better fit of the atlas, especially in the presence of anatomical variations induced by cortical or subcortical atrophy. Although a more precise method, manual nonlinear distortion of an atlas would require a time-intensive step of point-to-point matching of multiple landmarks in the atlas with those on the neuroimage obtained in the patient. We have recently developed a technique for automatic atlas integration with the individual patient's MR imaging space.⁹³ A labor-intensive tagging process is initially required for integration of the atlas with a model MR imaging data set. This process must be performed only once to produce a canonical atlas. For subsequent use, a computer-intensive automatic nonlinear image-matching algorithm^{19,21} can be used to fuse the model MR image with that of the patient, thus allowing precise automated atlas integration. The computerized atlas was initially integrated into a stereotactic surgical planning platform.⁹³ The platform allows visualization of stereotactic targets and surgical probes, lesion modeling, and intraoperative correlation of physiological responses with the MR imaging-atlas integrated anatomical space of the individual patient. In the present study, we used the integrated atlas to evaluate postoperative MR imaging data. On this basis we determined the stereotactic location and size of the thalamotomy lesion and its relationship to the thalamic nuclei. The lesions were evaluated within the standardized atlas space, and statistical comparisons were used to determine the relationship between clinical outcomes and lesion characteristics.

Clinical Material and Methods

Patient Population

The lesions were derived from a series of consecutive patients who underwent stereotactic procedures for movement disorders performed by one surgeon (A.F.S.) at the Montreal Neurological Institute and Hospital between April 1995 and October 1998. All patients were evaluated by a neurologist and neurosurgeon in the context of a surgical movement disorders clinic. In this study we included only

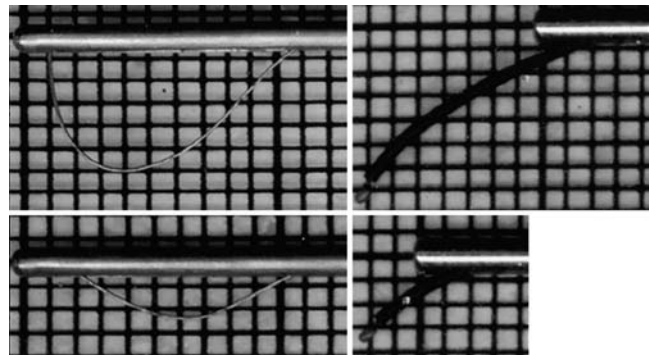


FIG. 1. *Left:* Photographs of the leukotome loop at its maximum (7 mm, *upper left*) and intermediate (*lower left*) extensions. *Right:* Photographs showing the curved stimulating electrode at its maximum (14 mm, *upper right*) and intermediate (*lower right*) extension.

patients who underwent thalamotomy for PD with functionally disabling tremor unresponsive to levodopa or anticholinergic agents. In an effort to keep clinical outcome criteria as uniform as possible, patients who underwent thalamotomy for essential tremor or dystonia were excluded. Also, patients who underwent pallidotomy and those who received deep brain stimulation to the thalamus, pallidum, or subthalamic nucleus were excluded from the present study.

Surgical Procedure

The stereotactic surgical procedure was performed after the patient received a local anesthetic agent. The procedural steps included frame application (Olivier Bertrand Tical frame⁸²; Tical Instruments, Montreal, QC, Canada), MR imaging, ventriculography, and, finally, physiological confirmation of the target prior to lesion generation. For thalamotomies, targets were centered on the Vim,⁴⁶ which is equivalent to the VLp of the thalamus.⁴⁸ Target localization was performed on the basis of multimodal imaging, including stereotactic ventriculography and stereotactic MR imaging. During surgery, physiological stimulation was performed using a retractable curved electrode, which allows exploration of a relatively large volume of tissue via a single trajectory (Fig. 1). The locations of motor fibers of the internal capsule and of the sensory thalamus were confirmed using a single electrode pass in most cases.¹¹ The stimulation parameters selected were 0.5 to 1 V, 60 Hz, and a 2-msec pulse duration. Optimal target location was further confirmed using high-frequency stimulation, resulting in tremor arrest that was generally apparent at the parameters 1 to 2 V, 185 Hz, and a 2-msec pulse duration.

In more recent cases, we used the atlas published by Schaltenbrand and Wahren,⁹¹ which was deformed in a nonlinear fashion into the stereotactic MR imaging space of the individual patient for preoperative and intraoperative planning of lesion localization, as previously described.⁹³ The stereotactic position of the tip of the curved electrode (Fig. 1) was modeled into the MR imaging-atlas integrated visualization platform. In most cases this method yielded an excellent correlation between responses obtained during physiological stimulation and either the anatomical border between the thalamus and motor fibers of the internal cap-

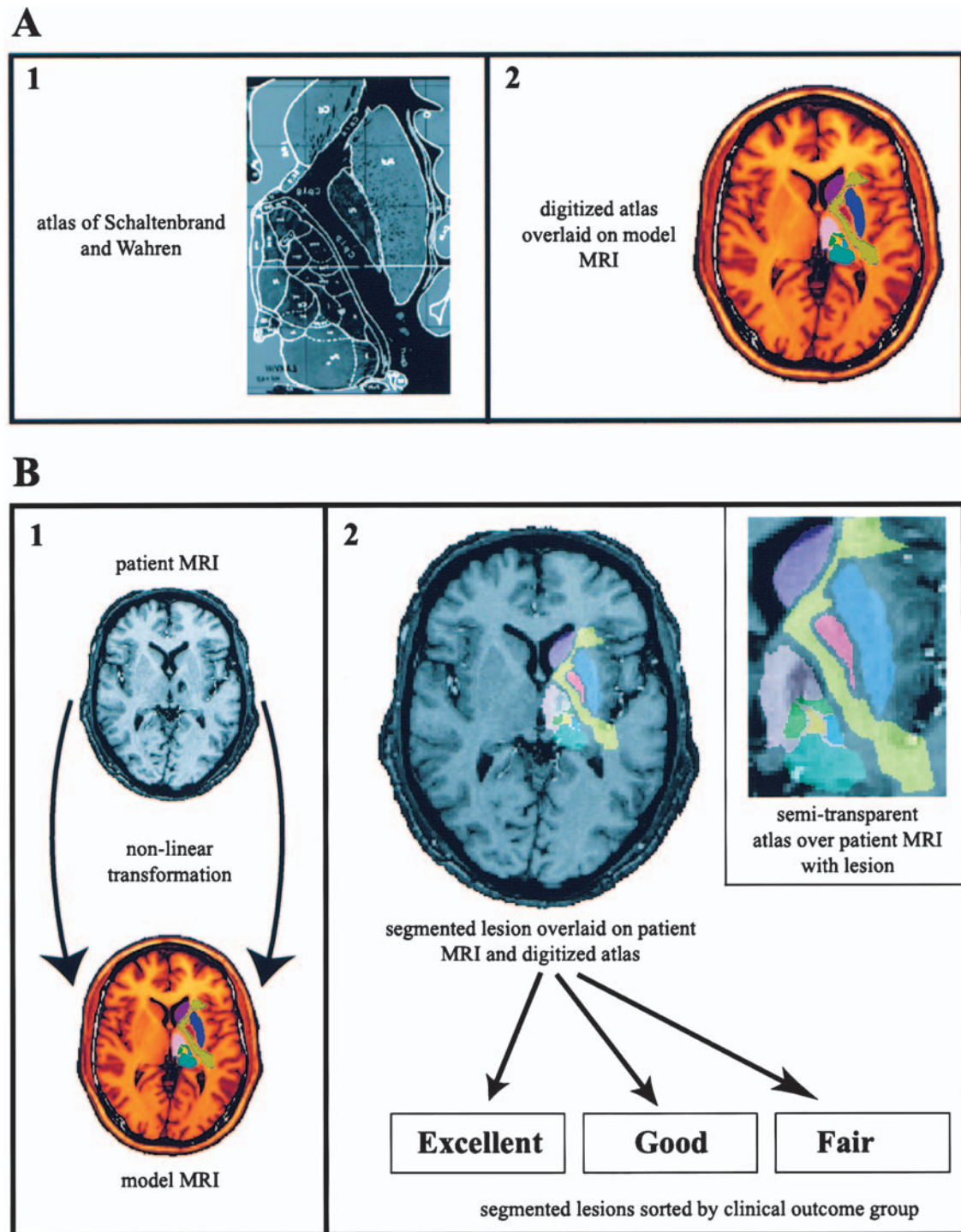


FIG. 2. Summary of the analysis procedure. A: Plates from the atlas of Schaltenbrand and Wahren⁹¹ (1) were previously digitized and integrated with a model MR image (MRI) that had a high signal-to-noise ratio (2). This set of steps was performed once. B: Subsequently, an MR image obtained in each patient was resampled to match the model MR image, based on the transformation generated by a nonlinear intensity-matching algorithm (1). Manually segmented lesions were then overlaid on the atlas and sorted into separate clinical outcome categories for statistical analysis (2).

sule, or the border between the Vim (VLp) and the sensory thalamus Vc (VP). Tailored lesions were created in a progressive, stepwise manner by using a graded retractable loop-shaped leukotome, with frequent intermittent clinical

examination.^{8,77,93} The leukotome is a curved wire loop that can be extracted at a variable diameter (1–7 mm) and rotated over the desired target volume, resulting in physical division of fibers and devascularization of the target (Fig. 1). In

Thalamotomy lesion evaluation

this manner, a tailored lesion can be created to conform to the desired target. Prior to step-wise lesioning, the proposed lesions were modeled and visualized in three dimensions on a computerized MR imaging-atlas integrated stereotactic platform, as previously described.⁹³ The average stereotactic target, defined at the tip of the leukotome and corresponding to the most ventral portion of the lesion, was in the AC-PC plane, 5.13 ± 0.82 mm (mean \pm SEM) behind the midpoint of the AC-PC line and 13.32 ± 0.93 mm (mean \pm SEM) lateral to the midpoint of the midline of the brain. The initial target was obtained from an evaluation of both MR imaging and ventriculographic coordinates. In general, the difference between stereotactic coordinates obtained using both imaging modalities was less than 2 mm. The final target was chosen after the evaluation of physiological responses. These progressive lesions were generally created in steps of 45° with a 4- to 7-mm extraction of the leukotome loop, depending on the proximity of the proposed lesion to the internal capsule or cutaneous sensory thalamus. Lateral stereotactic x-ray films were obtained during either stimulation or lesioning. Because the control x-ray films were obtained under stereotactic conditions identical to those used to obtain the ventriculogram, superimposition of the two x-ray films allowed immediate intraoperative confirmation of the position of probes with respect to the ventriculography-defined target. The control stereotactic x-ray films were also used to determine the proximity of the leukotome loop to the area at which the extracted curved monopolar stimulating electrode elicited sensory responses. Frequent clinical examination was performed during leukotome extraction in the posterior quadrant to ensure that cutaneous sensation remained intact. In general, lesions were made anterior to the sensory hand or face area. In cases in which immediate tremor relief was obtained, lesions in the posterior quadrants were generally limited to 5-mm leukotome extensions. In cases in which the tremor had a higher amplitude or was more resistant, the extent of the lesion created in the posterior quadrant was 7 mm. The method allowed generation of a wide variety of sizes and shapes of lesions conforming to the target structure and avoiding spillover into the internal capsule and cutaneous sensory thalamus.

Terminological Concerns

Our digitized stereotactic atlas is based on that published by Schaltenbrand and Wahren.^{91,93} In that atlas and an earlier one published by Schaltenbrand and Bailey,⁹⁰ Hassler's terminology was applied to thalamic nuclear divisions.^{45,46} More recently, a terminology designed to provide better homology between different primate species and to take into account recent data on chemical anatomy and connections of the thalamus was proposed by Jones and colleagues.^{48,70} We apply Hassler's terminology throughout this paper. For clarity, homologous nuclear subdivisions suggested by Jones and colleagues are indicated in parentheses throughout the text.

Clinical and Imaging Evaluation

All patients were initially examined by a neurologist and a neurosurgeon. Patients selected for surgery underwent a preoperative evaluation in which the Unified Parkinson's Disease Rating Scale²⁸ was applied, and also were exam-

ined by a neuropsychologist. Postoperative follow-up evaluation by the neurologist and neurosurgeon occurred at 6 to 8 weeks and 1 year after surgery. Follow-up neuropsychological examination occurred at 3 months and 1 year after surgery. For the purposes of this report, clinical outcomes at 6 to 8 weeks were assigned to four different categories similar to those used by previous authors.^{29,54} Tremor specific to the arm contralateral to the site of thalamotomy was evaluated at rest, with arms extended, and during repetitive finger-to-nose testing. Outcome categories were defined as follows: 1) excellent indicated no significant, clinically detectable tremor, with marked improvement in function; 2) good indicated a marked improvement in function and tremor amplitude, although some residual, clinically detectable tremor still remained; 3) fair indicated some improvement in tremor amplitude, but functionally significant residual tremor; and 4) no effect indicated no detectable change in tremor amplitude. In all cases MR imaging examinations were performed during the first 48 hours postoperatively (most within 24 hours). The images were acquired with the aid of a 1.5-tesla MR imaging system (ACS-2; Phillips Medical Systems, N.A., Bothell, WA) by using a 3D gradient echo sequence (TR 27 msec, TE 9 msec, flip angle 30° , $1 \times 1 \times 1.5$ -mm resolution, and two signal averages). The leukotome-induced lesions appeared hypointense on these T₁-weighted images with respect to surrounding brain. The images were analyzed in the following manner. First, a canonical MR imaging-based integrated atlas was created, as previously described.⁹³ Briefly, an image with a high signal-to-noise ratio was initially created for use as a model image set by averaging 27 image acquisitions of a single healthy human brain, which were registered to one another to a 0.1-mm accuracy.⁵¹ The model brain had an AC-PC length of 27 mm; a thalamic height, measured at the AC-PC midpoint, of 19 mm; and a third ventricular width, measured in the AC-PC plane, of 4 mm. A digitized version of the atlas of Schaltenbrand and Wahren⁹¹ (Fig. 2) was created and then tagged to this model brain by using homologous landmarks visible in both the atlas and on the MR image.⁹³ This entire procedure need be performed only once. The atlas was then applied to surgical planning and to lesion evaluation as part of the present study. An automated nonlinear warping algorithm based on intensity matching¹⁹ was used to generate the transformation between the MR image of each patient and the model MR image. In preparation for surgical planning, the inverse of the transformation was used to deform the atlas to fit the preoperative MR image of each individual patient. This resulted in atlas integration within the stereotactic space of the patient.⁹³

For this study, the forward transformation, generated by the same intensity-matching algorithm, was used to resample the MR image obtained in the patient to match the model brain and, hence, the atlas. This allowed all lesions to be objectively compared in a standard reference space. The integrated images were individually examined to determine the goodness of fit of the digitized atlas to the MR image obtained in each patient and to consider the position of the lesion with respect to the subnuclei. Individual lesion areas were manually segmented. Volumes of individual lesions were determined in the native MR imaging space. For group analysis, all lesions were considered to be left sided. This was achieved by matching any MR image that con-

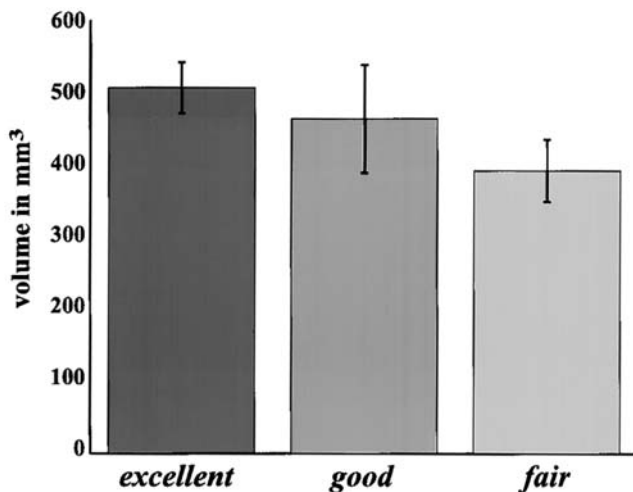


FIG. 3. Graph showing mean lesion volumes by clinical outcome group. The differences are not statistically significant.

tained right-sided lesions to a mirror image of the model MR image. Segmented lesions were then flipped to the left side, as a final step before the data were subjected to statistical analysis. Probabilistic maps for each clinical outcome category were then created by averaging together the individual segmented lesion volumes on a pixel-by-pixel basis. The centers of mass of individual lesions were calculated in the common reference space. Statistical comparisons were made of the lesion location or lesion volume to determine differences based on clinical outcome categories. The analysis procedure is summarized graphically in Fig. 2.

Statistical Analysis

Coordinates of the center of mass and volume measurements of segmented lesions were used for the statistical analysis. The coordinates of each pixel on the MR image were represented in millimeters as distance measurements from the origin, that is, the midpoint of the AC–PC line. In this coordinate system, the value of x increases from the left to the right side, the value of y increases from posterior to anterior, and the value of z increases from inferior to superior. Differences in spatial position were evaluated by assessing for statistically significant differences in the coordinates of lesion centers of mass as sorted by clinical outcome group. Because the longest distance between any group of lesions was not necessarily in line with standard axes, we also projected the coordinates of individual lesions along a line connecting the coordinate of the average lesion in each of the three outcome groups. We then determined whether the position along the line of projected coordinates of lesions was significantly different when any two groups were compared. The Kruskal–Wallis test and the Wilcoxon rank-sum test for post hoc analysis were used in the native coordinate analysis. The Wilcoxon rank-sum test, with the alpha level corrected for multiple comparisons, was used for the projection coordinate analysis. Differences in lesion volumes were also assessed using the Kruskal–Wallis test.

Initial visual analysis indicated that lesions differed in the degree to which they overlapped individual thalamic nuclei; we therefore analyzed the amount of overlap of each lesion with the Vim (VLp) and Vc (VP). Differences in overlap

volume by outcome group were assessed using the Kruskal–Wallis test and the Wilcoxon rank-sum test for post hoc analysis.

Results

Clinical Outcomes

A total of 35 thalamotomies were performed in patients with tremor-predominant PD.⁴ Cases with insufficient usable postoperative imaging data were excluded from the study; thus 25 patients who underwent 31 procedures were evaluated in this study. At the time of surgery, the ages of the patients ranged from 47 to 76 years (median age 62.5 years). Twenty patients were men and five were women. Fourteen lesions were located in the right hemisphere and 17 in the left hemisphere. Twenty-four lesions were created in patients who had not undergone thalamic surgery previously, three lesions were created for thalamotomy extension in cases in which recurrence of tremor appeared shortly after the first operation, and four thalamotomies were performed in patients who had undergone previous contralateral surgery.

All patients experienced excellent suppression of tremor, which was observed at the time of the operation. Different clinical outcomes were evident at the time of follow-up examinations. The 31 procedures evaluated in this report were divided according to clinical outcomes in the manner described in *Clinical Material and Methods*. Twenty-four lesions resulted in excellent clinical outcomes, four in good outcomes, three in fair outcomes, and no lesions were categorized as having no effect. All three lesions initially associated with fair outcomes and one of the four lesions correlated with good outcomes were subsequently extended within 3 months after the initial surgery, resulting in excellent outcomes in all cases. Of the lesions excluded from analysis due to insufficient usable postoperative imaging data, one primary lesion resulted in a good outcome, another primary lesion was associated with an excellent outcome, and two lesions were extensions resulting in excellent outcomes. Considering outcome as the final result of all surgical procedures, a reduction in tremor amplitude was achieved in all patients (89% excellent outcome and 11% good outcome), with improvement maintained at follow-up examinations performed at least 1 year after surgery.

Evaluation of the Lesion

In each patient the result of MR imaging–atlas integration was examined for goodness of fit. Integration of atlas structures with well-recognized subcortical landmarks on MR imaging, such as the thalamic border, internal capsule, caudate, and putamen, was considered excellent in all but three cases. Examination of those three cases revealed a minor discrepancy (< 2 mm) in the degree of overlap in the boundaries of these well-recognized subcortical structures. These three volumes were obtained in patients included in the excellent clinical outcome category. Lesions were evaluated with respect to their differences in volume, centers of mass, and degree of overlap with individual thalamic nuclei. In addition, subtraction analysis was performed on the basis of probabilistic maps generated for lesions in the different clinical outcome categories.

Thalamotomy lesion evaluation

TABLE 1

Centers of mass determined from lesion probabilistic maps*

Outcome Group	Coordinate (mm)		
	X	Y	Z
excellent	-13.4	-3.1	6.5
good & fair	-13.6	-0.6	5.4
essential lesion	-13.2	-5.1	6.7

* The locations of each of the probability density map centers of mass are shown as distance from the midpoint of the AC-PC line in the model MR image. See text for description of model MR image and definition of clinical outcome groups. Coordinates of the essential lesion were determined by subtraction analysis of probabilistic maps. Essential indicates a lesion volume that is required (but not necessarily sufficient) for excellent tumor relief.

Comparison of Lesion Volumes. A comparison of the average volume of lesions (Fig. 3) associated with each outcome category showed no statistically significant difference (Kruskal-Wallis test, $H = 1.8$, $p > 0.05$), although larger volumes were observed with lesions associated with better clinical outcomes.

Comparison of Centers of Mass. Coordinates of lesion centers of mass were compared in the three clinical outcome groups. The analysis revealed no statistically significant differences in x and z coordinates between groups. The y coordinate was located 3.1 ± 1.6 mm (mean \pm SD) posterior to the midpoint of the AC-PC line in the excellent outcome group, compared with 0.6 ± 1.6 mm (mean \pm SD) posterior to the midpoint in the suboptimal outcome (good and fair) groups. Statistically significant differences were noted ($H = 10.2$, $p < 0.05$) in the y coordinate when a comparison was made between good and excellent outcome groups or between fair and excellent outcome groups. No significant difference was noted in the y coordinate between fair and good outcome categories. The x coordinate of the centers of mass of lesions in the excellent outcome group was 13.4 ± 1.6 mm (mean \pm SD) lateral to the midline, close to the x coordinate of suboptimal lesions, which was 13.6 ± 1.1 mm (mean \pm SD) lateral to the midline. The z coordinate in the excellent group was 6.5 ± 1.5 mm (mean \pm SD) above the AC-PC plane compared with 5.4 ± 1.8 mm above the plane in the suboptimal outcome groups. Note that average coordinates correspond to the center of the lesion, thus explaining why the z coordinate lies above the chosen target, which represents the tip of the leukotome probe (Fig. 1).

In addition to an analysis of the native coordinate space, a projection coordinate analysis was also performed. Locations of centers of mass of individual lesions were projected along a line connecting the two average lesion coordinates in each category compared, and the Kruskal-Wallis test and Wilcoxon rank-sum post hoc test were then applied, as described in *Clinical Material and Methods*. Once again, a significant difference was found between positions of lesions associated with good and excellent outcomes, and between locations of lesions correlated with fair and excellent outcomes ($p < 0.05$). No difference was detected between positions of lesions linked with good and fair outcomes. The coordinates of the centers of mass of the lesions derived from probabilistic maps expressed relative to the midpoint of the AC-PC line are shown in Table 1. Lesions

TABLE 2

Mean overlap of lesions with thalamic subnuclei*

Outcome Group	Nucleus Overlapped (mm ³)	
	Vim	Vc
excellent	53.2 (23.6%)	17.1 (3.2%)
good & fair	13.8 (6.1%)	2.4 (0.45%)
p value	0.0046	0.0172

* Evaluated using the Fisher exact test.

resulting in good outcomes, on average, were located 3.73 mm from those resulting in excellent outcomes in the antero-inferolateral direction. Lesions resulting in fair outcomes, on average, were located 2.05 mm from those resulting in excellent outcomes, in the anterosuperomedial direction. It is clear from both analyses that lesions created in patients in suboptimal outcome categories were located anterior to those created in patients in the excellent outcome category. The probabilistic maps of lesions in each category are shown overlaid on the atlas in Fig. 4.

Degree of Overlap With Individual Thalamic Nuclei. The probabilistic maps demonstrate that lesions in different outcome categories varied in distribution with respect to thalamic nuclei. All lesions associated with excellent outcomes and all but one correlated with suboptimal outcomes involved a portion of the Vim (VLp). Sixty-seven percent of lesions associated with excellent outcomes and 30% of those linked with good or fair outcomes involved more than 10% of the Vim (VLp) by volume. Lesions leading to suboptimal outcomes showed less overlap with the Vim (VLp) than those leading to excellent outcomes. A significant number of lesions also involved the rostral portion of the Vc (VP), which likely corresponded to the Vcae (VPLa). Whereas 83% of lesions resulting in excellent outcomes involved the Vc, only 43% of lesions resulting in good or fair outcomes involved this nucleus. Fifty percent of lesions leading to excellent outcomes involved more than 2% of the volume of the Vc, whereas lesions leading to other outcomes did not display this degree of encroachment on the nucleus. A comparison of the three outcome groups revealed no significant difference in the mean volumes of lesion overlap of either the Vc or the Vim (Kruskal-Wallis test). A statistically significant difference was apparent, however, when patients in the fair and good outcome categories were grouped and compared with those in the excellent outcome category. Wilcoxon rank-sum tests revealed that lesions in patients in the excellent outcome group showed significantly more overlap of both the Vim ($p < 0.01$) and Vc ($p < 0.05$), compared with lesions in patients in both good and fair outcome groups. These results are summarized in Table 2.

Subtraction Analysis of Probabilistic Maps. To establish specifically which thalamic nuclei are necessary targets for excellent outcome, we generated probabilistic maps of lesions in each category and then performed a subtraction analysis. Because the locations of lesions associated with good and fair outcome categories could not be distinguished statistically, their volumes were averaged together and subtracted from the volumes of lesions correlated with the excellent outcome category. The location of this subtracted lesion is illustrated in Fig. 4. The coordinates of the

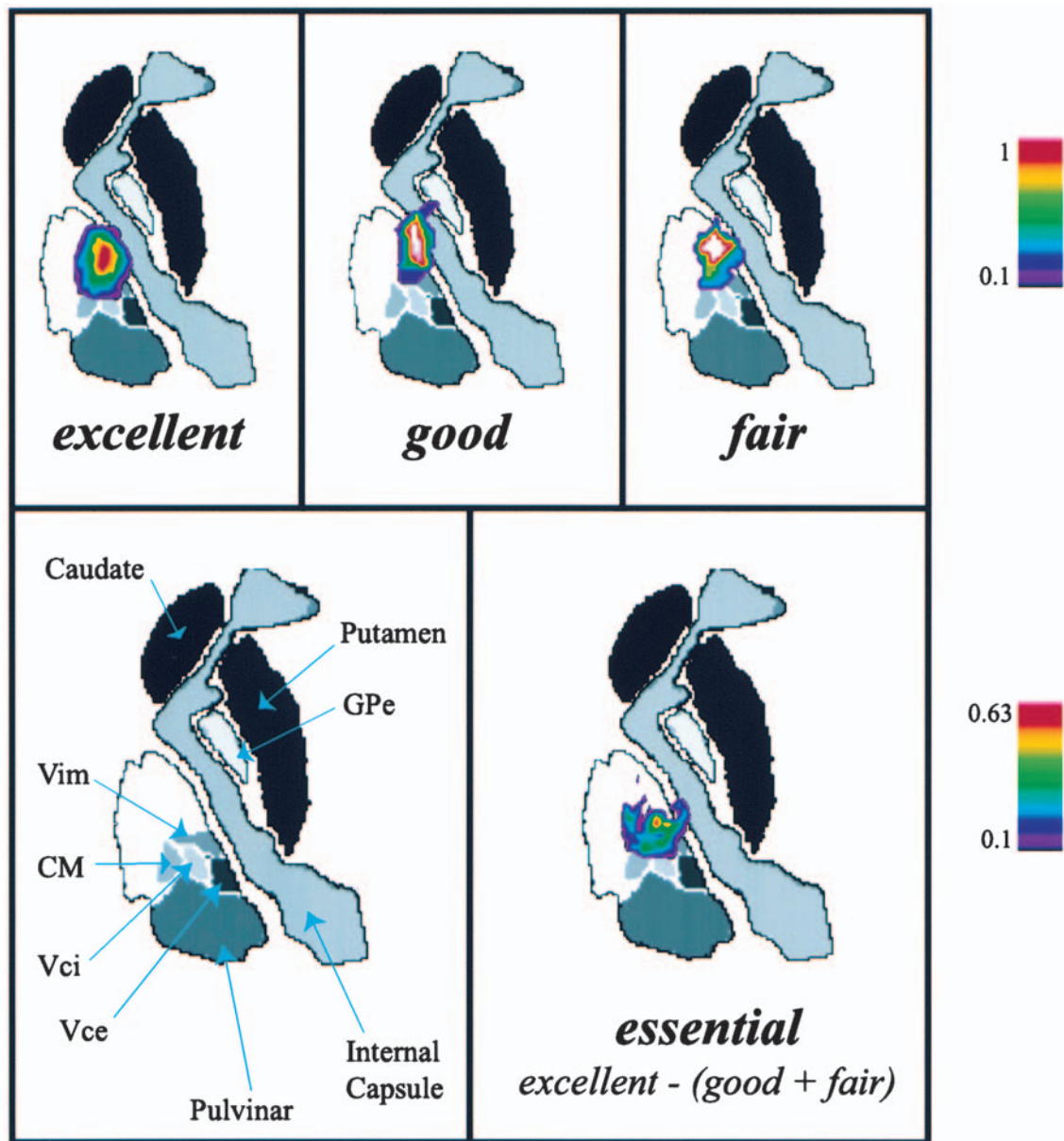


FIG. 4. Probabilistic maps for the three outcome categories—excellent, good, and fair—shown in axial slices centered at the coordinates of the center of mass of the essential lesion. The color bars at the right correspond to the probability of each pixel being represented in each lesion. The essential lesion represents a positive result of the pixel-wise subtraction of lesions from the good and fair outcome categories from the lesion from the excellent outcome category. GPe = globus pallidus externus. The essential lesion is necessary, but may not be sufficient for an excellent clinical outcome.

center of mass of this lesion, relative to the midpoint of the AC–PC line, are given in Table 1. The results of the subtraction analysis suggest an essential lesion volume that is required (but not necessarily sufficient) for excellent tremor relief. This essential volume involves not only the Vim (VLp), but also extends into the anterior and anterodorsal portions of the Vc or Vcae (VPLa). The latter area is coextensive with the shell of the Vc, which includes proprioceptive or kinesthetic units.^{10,12,42,55,56,65,79}

Discussion

Renewed interest in stereotactic neurosurgery for the

treatment of movement disorders has led to numerous reports of clinical outcomes associated with diverse treatment strategies.^{29,33,40,54,94} In addition to clinical data, rigorous anatomical postoperative evaluation of the stereotactic placement of long-term stimulating electrodes or lesions is essential for a valid comparison of surgical methods. So far little detailed anatomical information has accompanied the results of clinical efficacy studies. The paucity of studies of anatomical–clinical correlation may be due to a lack of systematic postoperative imaging or autopsy studies, variable length between surgical procedures and postoperative brain imaging, and difficulties encountered when comparing lesions of variable size and configuration. We have devel-

Thalamotomy lesion evaluation

oped a unique method for evaluating subcortical lesions in a common reference space. This method was used systematically to correlate clinical outcome of thalamotomy for tremor with lesion location, volume, and configuration. A subcortical atlas of deep brain structures was integrated into the standardized space of MR images, allowing a detailed comparison. The analysis revealed statistically significant differences in lesion location between excellent and good, and excellent and fair outcome categories. On average, lesions associated with excellent outcomes were located more posteriorly than those in the other two outcome groups. Subtraction analysis revealed that lesions associated with excellent outcomes necessarily involved the interface of the Vim (VLp) and Vc (VP). We discuss the significance of these findings with reference to clinical results, terminology, and anatomical–physiological correlations. We also discuss the use of our unique probabilistic method for evaluating subcortical lesions with reference to an MR imaging–based integrated atlas.

Methods for the Study of Lesion Characteristics

Postmortem histological studies of lesion location^{7,41} or deep brain stimulator lead placement¹⁷ allows the most direct analysis of optimal targets. Histological comparisons of postmortem anatomy and clinical outcomes^{7,22,44,47,72} have contributed to the choice of the Vim (VLp) as the main surgical target used for relief of tremor associated with PD. This approach is limited by a possible postmortem artifact, sparse databases, and variable age of the lesions at the time of examination. Intended targets have also been correlated with patient outcomes,^{27,43,59} and the results have contributed significantly to modern surgical procedures. The latter approach is limited by a possible mismatch between the intended and actual lesions with respect to location, size, and configuration. Furthermore, focusing on the coordinates of the center of the intended lesion underestimates the significance of involvement of structures at the lesion's periphery. As a refinement of this approach, attempts have been made to predict volumes of radiofrequency-induced lesions based on formula-modeling heat deposition in tissue.^{23,49} Electrophysiological information obtained at surgery from microelectrode recordings has also been used to define the placement of stereotactic lesions within the known functional anatomy of the human thalamus more precisely.^{55,57,66,99} Nevertheless, this approach is also limited by a lack of correlation between clinical outcome and final lesion volume and configuration.

More recently, modern imaging procedures have been used to examine the postoperative location, shape, and volume of the lesion. Clinically, x-ray films or ventriculographic images of intraoperative instrument placement have been used to estimate the location of the lesion⁹⁷ and to correlate this with clinical outcome.²⁷ Postoperative image evaluation performed using CT or MR imaging is the current method of choice for confirming target location, but this approach is limited by the spatial resolution and contrast-to-noise ratio of available imaging methods. Recently, postoperative MR imaging has been used to assess the position of the lesion with respect to the AC–PC line⁸⁴ and to measure lesion volumes generated using gamma knife or radiofrequency techniques.^{30,101} Although there are no systematic studies of MR imaging–based localization of thal-

amotomy lesions, the characteristics of pallidotomy have been examined.^{18,36,37} In these studies targets were localized relative to the midpoint of the AC–PC line, and linear image registration and scaling principles were implemented. Using this method, authors of a recent analysis of a series of patients who underwent pallidotomy demonstrated a relationship between lesion location and clinical outcomes.³⁷

Even with optimal resolution, current imaging does not allow identification of anatomical boundaries within the thalamus. To this end, standardized atlases of subcortical anatomy may be combined with neuroimaging to increase subcortical detail on postoperative images.^{2,15,35,58,76,93} The most common application of this technique involves determining the distance between the AC and the PC on postoperative images, and then scaling atlas slices to matching imaging planes.^{2,58} Computerized tomography scanning–based atlas integration has been used in this manner to examine thalamotomy characteristics.¹⁰⁴ A similar linear scaling method can also be applied in three dimensions after interpolating atlas slices into a 3D volume.^{34,83} Although these modern studies, in which researchers implement image-based lesion evaluation with linear scaling of atlases, represent significant advances, errors in interpretation may still result because the researchers do not account for nonlinear variations in the structure of individual brains.

Image Analysis Technique

We have used a novel, automated, nonlinear fitting algorithm to plan surgical procedures, for intraoperative guidance,⁹³ and to evaluate the location of a lesion or a deep brain stimulator. The technique is easy to apply, increases the accuracy of localization, and is useful for evaluating individual patients and performing group analyses. The relatively large number of patients who were studied allowed us to demonstrate a difference in the position of the lesion by tremor outcome group, which has not been clearly demonstrated in previous studies.⁴³ Our study is also unique because of our use of nonlinear registration for the study of surgical lesions in a standardized space 3D MR imaging–based atlas integration for statistical evaluation of lesion location within the thalamic nuclei, and correlation between both the size and configuration of thalamic lesions observed on MR images and clinical outcomes.

Imaging-based methods have a number of limitations. Physical properties of the patient or the imaging unit can introduce distortions into the spatial characteristics of the MR image,⁹⁶ which may affect accuracy. Unlike histological methods, which can be used to define the reference structure, our algorithm relies on detection of relative differences in signal intensities on MR images for nonlinear transformation of images of the individual patient's brain into images of a reference brain.¹⁹ Theoretically, individual variations in brain anatomy that lie below the resolution of MR imaging may introduce error during registration. Furthermore, although the automated algorithm that generates the nonlinear transformation has been extensively tested in healthy brains,¹⁹ the quality of registration may be influenced by factors such as a movement artifact or intracranial air. For this reason, a careful review of each atlas integration is necessary when using automatic algorithms. Despite these limitations, automated nonlinear image-matching algorithms represent an advance over simple linear transfor-

mations.¹⁹⁻²¹ These algorithms make no a priori assumption about deformation in subcortical structure based on a limited number of points (for example, the AC or the PC). Furthermore, automated algorithms allow for rapid integration of MR imaging data sets, avoiding laborious point-to-point matching by the user. In comparison with linear scaling, nonlinear matching may be especially important when dealing with MR imaging data sets that have been altered by pathological conditions, such as cortical and subcortical atrophy associated with aging. Our technique may therefore be especially suited to the creation of disease-based atlases designed for use during therapeutic interventions. Automated nonlinear image registration and atlas integration is also applicable to evaluation of other subcortical stereotactic procedures, determination of the position of pathological lesions,^{19,20} and characterization of the anatomical significance of functional imaging data sets. Finally, we are currently using similar automated atlas integration methods to create a functional database of electrophysiological responses obtained during stereotactic functional neurosurgery.

Efficacy of Thalamotomy for Tremor: Correlation With the Site of the Lesion

Thalamotomy is a well-established, effective treatment strategy for relief of tremor.⁴⁰ In cases of PD, lesions centered on the Vim (VLp) are most effective for relief of tremor, whereas more anterior lesions involving the Vop (VLa) result in relief of rigidity.^{29,40,81} The reported effectiveness of unilateral thalamotomy for tremor varies between 45 and 92%, with 7 to 15% of patients requiring additional procedures to achieve optimal results.^{29,33,54,73,100} In our series, all patients initially experienced relief of tremor during surgery. Evaluations performed in 31 patients 4 to 6 weeks after thalamotomy revealed excellent (77% of patients), good (13% of patients), or fair (10% of patients) relief of tremor. Fifty-seven percent of patients in the good or fair outcome categories underwent lesion extension within 3 months after the initial surgery, resulting in conversion of their cases to the excellent outcome category. A lasting reduction in tremor amplitude (evaluated at least 1 year after surgery) was achieved in all patients in the series, with 89% of cases in the excellent outcome category and 11% in the good outcome category.

Our technique involves creating tailored lesions centered on the Vim.^{14,93} The lateral limit of the lesions is determined by mapping the motor fibers of the internal capsule by using a retractable monopolar stimulating electrode. The intent is to include most of the lateral portion of the Vim (VLp) in the lesion, but to avoid the internal capsule. The posterior limit of the lesion is delineated by mapping the cutaneous sensory thalamus, which is also accomplished using the curved monopolar electrode.¹³ Here the goal is to extend the Vim (VLp) lesion immediately rostral to the sensory cutaneous thalamus, including the Vcae (VPLa) and the Vcai (rostral VPM) (the kinesthetic thalamic territory), but avoiding numbness. The size of tailored lesions is determined, in part, by the degree of reduction in tremor observed during intraoperative clinical examination.

All lesions involved motor areas located anterior to the Vim (VLp), which were targeted in this PD patient population to reduce rigidity^{29,47} and, possibly, dyskinesias.⁷⁵ We

demonstrated the precise location, volume, and configuration of individual lesions, and our imaging environment allowed a statistical comparison of groups of lesions associated with distinct clinical outcomes. The most effective lesions were located significantly more posteriorly within the thalamus, compared with less effective lesions. With atlas integration, we were also able to describe the extent to which lesions involved the Vim (VLp), Vc (VP), and surrounding areas. Ninety-seven percent of the lesions in our study involved the Vim (VLp). The analysis also showed that lesions in suboptimal outcome groups involved a smaller volume of Vim (VLp) than lesions associated with an excellent outcome (Table 2). A significant number of lesions also involved the rostral portion of the Vc (VP), likely corresponding to the Vcae (VPLa). Table 2 demonstrates that lesions in cases comprising the excellent outcome category involved a significantly greater percentage of the Vc than lesions in cases forming the other two groups. These data support the notion that extension of the lesion into the anterior portion of the Vc is important to achieve an excellent outcome. This is further supported by the results of the subtraction analysis, which demonstrate that lesions associated with excellent outcomes have an essential volume, which includes the posterior portion of the Vim (VLp) and the anterior portion of the Vc (VPLa). Although a lesion of this essential area is necessary to achieve an excellent outcome, it may not be sufficient. Lesions located in the more rostral portion of the Vim may also be required for adequate relief of tremor and may be associated with an additional salutary effect on rigidity.^{22,50,74}

A comparison of the total volume of lesions in each outcome category revealed no statistically significant difference. Our data indicate that lesion location, independent of lesion size, determines the degree of tremor suppression, although it is possible that this conclusion is limited by reduced statistical power due to the small number of lesions in suboptimal outcome categories. The average lesion volume in the present series is larger than those of other reports identifying the minimum effective volume of thalamotomy lesions for tremor.^{43,49,66} It is important, however, to note that our tailored lesion technique involves use of a leukotome, whereas most reports on lesion volume cover radiofrequency-generated lesions. The physiological effect of heat-induced lesions may extend beyond that of induced necrosis,^{23,103} thus underestimating the effective lesion volume. Furthermore, in the present study we report lesion volumes measured on MR images, which may be significantly larger than those reported in previous studies in which they were measured on CT scans.^{25,69,102} Finally, lesions may retract significantly with time, possibly accounting for the fact that lesions detected on images obtained during the early postoperative period are larger than those measured on images obtained at later time points^{25,69,102} or at autopsy. Early postoperative imaging may also identify edema and local reaction as a component of the MR imaging signal at the lesion site. These time-dependent effects have been clearly documented in cases in which the lesions were induced by radiofrequency.^{25,102} Edema is not likely to be an important component in the leukotome-induced lesions presented here, because imaging was performed within 24 hours after surgery in most cases.²⁵ The relatively large size of the lesions in our patients with PD also reflects the desire to include the VLa for the control of rigidity,^{22,50,74} in addition to

Thalamotomy lesion evaluation

more posterior areas of the ventral thalamus targeted for control of tremor. The results of our study indicate that tailoring lesions to target structures of interest is more important than lesion volume in predicting clinical outcome. Furthermore, the tailored lesioning technique, accompanied by physiological stimulation and 3D lesion planning, allows for avoidance of critical neighboring structures such as the internal capsule and cutaneous sensory thalamus, thus reducing the incidence of potential complications such as numbness, dysarthria, or motor weakness.

Pathophysiological Significance of the Effective Target for Relief of Tremor

The anatomical data obtained in this study contribute to our understanding of the functional anatomy of tremor. The ventral thalamus may be divided into anterior, intermediate, and posterior parts.^{4,5,52,53} With respect to the motor thalamus, homological studies in nonhuman primates have broadly demonstrated segregated pallidal and cerebellar recipient sectors.^{87,88,95} Afferents from the internal pallidal segment distribute to the Voa and Vop (VL_a), and the CM. The thalamic territory that receives afferents from the deep cerebellar nuclei includes the Voi, Vim, Zim and Dim (VL_p), and the CM. The pallidal recipient areas of the ventral thalamus send efferents primarily to premotor and supplementary motor areas, whereas the cerebellar recipient sectors project mainly to the primary motor cortex.^{87,88,95} In nonhuman primates, the primary sensory thalamus—Vc (mainly VPL and VPM)—may be subdivided electrophysiologically into an anterodorsal shell containing neurons with proprioceptive or kinesthetic properties^{56,71} (the Vca_e or VPL_a), and a posterior and ventral core containing cutaneous responsive units.^{56,85} A similar electrophysiological organization appears to exist in humans, including proprioceptive or kinesthetic units dispersed over an anterior and dorsal shell,^{39,55,64,65,81} and a cutaneous responsive core.⁹² The majority of kinesthetic responsive units appear to be within the Vca_e and the Zc (the VPL_a), a thin shell that is approximately 2 mm thick.^{1,55,64,65,81,90}

Data from physiological unit recording studies of PD in humans reveal cells in the ventral thalamus that are characterized by rhythmic burst activity. Some of these bursting units are synchronous with peripheral tremor.^{1,26,38,55} Other rhythmic cells, burst firing at 3 to 6 Hz, are located more rostrally compared with cells that are time locked with the contralateral peripheral limb tremor.^{42,55} These cells do not fire as regularly as their more caudal, tremor-locked counterparts and are likely to be located in the Vim (VL_p), Vop (VL_a), and, possibly, the Voa (VL_a).⁵⁵ In many cases, units demonstrating rhythmic burst spike activity also respond to passive or active joint movement, presumably related to activation of muscle spindles. These neurons do not respond to light touch and, rather, may receive sensory inputs either indirectly via spinocerebellar pathways or more directly via the dorsal column–lemniscal system.^{64,68} Kinesthetic cells^{78,80} are largely coextensive with time-locked tremor cells and are located mainly in the lateral Vim (VL_p) and in the most rostral portion of the Vc (VPL_a).^{10,12,42,55,65} Although thalamic kinesthetic response cells and tremor cells are consistently located rostral to the tactile responsive zone, the extent to which tremor-evoked kinesthetic cells occupy the Vim (VL_p) or the Vc (VP) in the human thalamus remains controversial.^{9,24,31,38,55,79,98}

In the present anatomical study we localized effective lesions mainly to the Vim (VL_p) and the most rostral portion of the Vc (VPL_a). Interestingly, all lesions also involved thalamic territories anterior to the Vim (VL_p), areas comprising the Vop (VL_a) and even the Voa (VL_a). These areas correspond to the pallidal recipient sector and also contain rhythmic bursting cells, although they are usually not tremor locked.^{14,65} Lesions in this more rostral area correlate with relief of rigidity,^{29,81} emphasizing the importance of pallidothalamic efferents in the pathogenesis of this symptom of PD. Subtraction analysis revealed that lesions that were most effective for relief of tremor involved the posterior portion of the Vim (VL_p) and the most rostral portion of the Vc (VPL_a). In fact, a significantly greater proportion of lesions associated with excellent outcome involved the Vca_e, corresponding to an area containing a high proportion of proprioceptive units. Ultimately, a collection of tremor cells distributed within thalamic areas anterior to the cutaneous responsive tactile sector is likely to be important for adequate relief of tremor.

Conclusions

Analysis of thalamotomy lesions placed stereotactically for relief of parkinsonian tremor revealed that optimal lesions associated with excellent outcomes are located more posteriorly than lesions correlated with suboptimal outcomes, independent of the size of the lesion. Atlas integration with the lesion evaluation, which is performed using a probabilistic approach, demonstrated that inclusion of the interface of the Vim (VL_p) with the anterior Vc (VPL_a) is necessary for an excellent outcome. This finding emphasizes the importance of the proprioceptive thalamus in the pathophysiology of parkinsonian tremor. In view of the variety of procedures currently applicable to movement disorders, precise anatomical characterization of the lesion or stimulator placement within the thalamus or basal ganglia will be helpful in evaluating the clinical indications for each treatment strategy. Use of the automated nonlinear image-matching algorithm for atlas integration has wide applicability beyond functional neurosurgery, including analysis of pathological lesions and generation of functional activation databases.

Disclaimer

None of the authors has any financial interest in the techniques presented here.

References

1. Albe-Fessard D, Arfel G, Guiot G, et al: Thalamic unit activity in man. **Electroencephalogr Clin Neurophysiol (Suppl 25)**:132, 1967
2. Alesch F, Koos WT: Computer-assisted multidimensional atlas for functional stereotaxy. **Acta Neurochir 133**:153–156, 1995
3. Alesch F, Pinter MM, Hellscher RJ, et al: Stimulation of the ventral intermediate thalamic nucleus in tremor dominated Parkinson's disease and essential tremor. **Acta Neurochir 136**:75–81, 1995
4. Asanuma C, Thach WR, Jones EG: Anatomical evidence for seg-

- regated focal groupings of efferent cells and their terminal ramifications in the cerebellothalamic pathway of the monkey. **Brain Res** **286**:267–297, 1983
5. Asanuma C, Thach WT, Jones EG: Distribution of cerebellar terminations and their relation to other afferent terminations in the ventral lateral thalamic region of the monkey. **Brain Res** **286**:237–265, 1983
 6. Bakay RA, Starr PA, Vitek JL, et al: Posterior ventral pallidotomy: techniques and theoretical considerations. **Clin Neurosurg** **44**:197–210, 1997
 7. Beck E, Bignami A: Some neuro-anatomical observations in cases with stereotactic lesions for the relief of parkinsonism. **Brain** **91**:589–618, 1968
 8. Bertrand C, Martinez N: An apparatus and technique for surgery of dyskinesias. **Neurochirurgica** **2**:36–46, 1959
 9. Bertrand C, Martinez SN, Hardy J: Electrophysiological studies of the human thalamus and adjoining structures. **J Neurol Neurosurg Psychiatry** **26**:552, 1963 (Abstract)
 10. Bertrand G: Discussion: studies of the human thalamus. **Brain Behav Evol** **6**:210–214, 1972
 11. Bertrand G, Blundell J, Musella R: Electrical exploration of the internal capsule and neighboring structures during stereotaxic procedures. **J Neurosurg** **22**:333–343, 1965
 12. Bertrand G, Jasper H: Microelectrode recording of unit activity in the human thalamus. **Confin Neurol** **26**:205–208, 1965
 13. Bertrand G, Jasper H, Wong A: Microelectrode study of the human thalamus: functional organization in the ventro-basal complex. **Confin Neurol** **29**:81–86, 1967
 14. Bertrand G, Jasper H, Wong A, et al: Microelectrode recording during stereotactic surgery. **Clin Neurosurg** **16**:328–355, 1969
 15. Bertrand G, Olivier A, Thompson CJ: The computerized brain atlas: its use in stereotaxic surgery. **Trans Am Neurol Assoc** **98**:233, 1973
 16. Bronstein JM, DeSalles A, DeLong MR: Stereotactic pallidotomy in the treatment of Parkinson disease: an expert opinion. **Arch Neurol** **56**:1064–1069, 1999
 17. Caparros-Lefebvre D, Ruchoux MM, Blond S, et al: Long-term thalamic stimulation in Parkinson's disease: postmortem anatomical study. **Neurology** **44**:1856–1860, 1994
 18. Cohn MC, Hudgins PA, Sheppard SK, et al: Pre- and postoperative MR evaluation of stereotactic pallidotomy. **AJNR** **19**:1075–1080, 1998
 19. Collins DL, Evans AC: ANIMAL: validation and applications of non-linear registration-based segmentation. **Int J Pattern Recog Artificial Intelligence** **11**:1271–1294, 1997
 20. Collins DL, Holmes CJ, Peters TM, et al: Automatic 3D model-based neuro-anatomical segmentation. **Hum Brain Mapp** **3**:190–208, 1995
 21. Collins DL, Neelin P, Peters TM, et al: Automatic 3D intersubject registration of MR volumetric data in standardized Talairach space. **J Comput Assist Tomogr** **18**:192–205, 1994
 22. Cooper IS, Samra K, Bergmann L: The thalamic lesion which abolishes tremor and rigidity of Parkinsonism: a radiologico-clinico-anatomic correlative study. **J Neurol Sci** **8**:69–84, 1969
 23. Cosman ER, Nashold BS, Bedenbaugh P: Stereotactic radiofrequency lesion making. **Appl Neurophysiol** **46**:160–166, 1983
 24. Crowell RM, Perret E, Siegfried J, et al: 'Movement units' and 'tremor phasic units' in the human thalamus. **Brain Res** **11**:481–488, 1968
 25. De Salles AA, Brekhus SD, De Souza EC, et al: Early postoperative appearance of radiofrequency lesions on magnetic resonance imaging. **Neurosurgery** **36**:932–936, 1995
 26. Duval C, Panisset M, Bertrand G, et al: Evidence that ventrolateral thalamotomy may eliminate the supraspinal component of both pathological and physiological tremors. **Exp Brain Res** **132**:216–222, 2000
 27. Fager CA: Evaluation of thalamic and subthalamic surgical lesions in the alleviation of Parkinson's disease. **J Neurosurg** **28**:145–149, 1968
 28. Fahn S, Elton RL, Members of the UPDRS Development Committee: Unified Parkinson's Disease Rating Scale, in Fahn S, Marsden CD, Goldstein M, et al (eds): **Recent Developments in Parkinson's Disease**. Florham Park, NJ: Macmillan Healthcare Information, 1987, Vol 2, pp 153–163
 29. Fox MW, Ahlskog JE, Kelly PJ: Stereotactic ventrolateralis thalamotomy for medically refractory tremor in post-levodopa era Parkinson's disease patients. **J Neurosurg** **75**:723–730, 1991
 30. Friehs GM, Noren G, Ohye C, et al: Lesion size following gamma knife treatment for functional disorders. **Stereotact Funct Neurosurg** **66** (Suppl 1):320–328, 1996
 31. Fukamachi A, Oye C, Narabayashi H: Delineation of the thalamic nuclei with a microelectrode in stereotaxic surgery for parkinsonism and cerebral palsy. **J Neurosurg** **39**:214–225, 1973
 32. Gabriel EM, Nashold BS Jr: Evolution of neuroablative surgery for involuntary movement disorders: an historical review. **Neurosurgery** **42**:575–591, 1998
 33. Gildenberg PL, Tasker RR, Franklin PO (eds): **Textbook of Stereotactic and Functional Neurosurgery**. New York: McGraw-Hill Health Professionals Division, 1998
 34. Giorgi C, Broggi G, Garibotto G, et al: Three-dimensional neuro-anatomic images in CT-guided stereotaxic neurosurgery. **AJNR** **4**:719–721, 1983
 35. Greitz T, Bohm C, Holte S, et al: A computerized brain atlas: construction, anatomical content, and some applications. **J Comput Assist Tomogr** **15**:26–38, 1991
 36. Gross RE, Lombardi WJ, Hutchison WD, et al: Variability in lesion location after microelectrode-guided pallidotomy for Parkinson's disease: anatomical, physiological, and technical factors that determine lesion distribution. **J Neurosurg** **90**:468–477, 1999
 37. Gross RE, Lombardi WJ, Lang AE, et al: Relationship of lesion location to clinical outcome following microelectrode-guided pallidotomy for Parkinson's disease. **Brain** **122**:405–416, 1999
 38. Guiot G, Albe-Fessard D, Arfel G, et al: Investigations électrophysiologiques en chirurgie stéréotaxique. **Rev Neurol** **107**:84–86, 1962
 39. Guiot G, Albe-Fessard D, Arfel G, et al: Représentation et organisation de la somesthésia dans le noyau ventral postérieur de l'homme. **Rev Neurol** **109**:465–467, 1963
 40. Hallett M, Litvan I: Evaluation of surgery for Parkinson's disease: a report of the Therapeutics and Technology Assessment Subcommittee of the American Academy of Neurology. The Task Force on Surgery for Parkinson's Disease. **Neurology** **53**:1910–1921, 1999
 41. Hanieh A, Maloney AF: Localization of stereotaxic lesions in the treatment of parkinsonism: a clinico-pathological comparison. **J Neurosurg** **31**:393–399, 1969
 42. Hardy TL, Bertrand G, Thompson CJ: Thalamic recordings during stereotactic surgery. I. Surgery topography of evoked and nonevoked rhythmic cellular activity. **Appl Neurophysiol** **42**:185–197, 1979
 43. Hariz MI: Correlation between clinical outcome and size and site of the lesion in computed tomography guided thalamotomy and pallidotomy. **Stereotact Funct Neurosurg** **54/55**:172–185, 1990
 44. Hartmann-von Monakow K: Histological and clinical correlations in 29 Parkinson patients with stereotaxic surgery. **Confin Neurol** **34**:210–217, 1972
 45. Hassler R: Anatomy of the thalamus, in Schaltenbrand G, Bailey P (eds): **Introduction to Stereotaxis With an Atlas of the Human Brain**. Stuttgart: Thieme, 1959, pp 230–290
 46. Hassler R: Architectonic organization of the thalamic nuclei, in Schaltenbrand G, Walker AR (eds): **Stereotaxy of the Human Brain. Anatomical, Physiological, and Clinical Application, ed 2**. Stuttgart: Thieme, 1982, pp 140–180
 47. Hassler R, Mundinger F, Riechert T: Correlations between clinical and autoptic findings in stereotaxic operations of parkinsonism. **Confin Neurol** **26**:282–290, 1965

Thalamotomy lesion evaluation

48. Hirai T, Jones EG: A new parcellation of the human thalamus on the basis of histochemical staining. **Brain Res Brain Res Rev** 14:1–34, 1989
49. Hirai T, Miyazaki M, Nakajima H, et al: The correlation between tremor characteristics and the predicted volume of effective lesions in stereotaxic nucleus ventralis intermedialis thalamotomy. **Brain** 106:1001–1018, 1983
50. Hirato M, Ishihara J, Horikoshi S, et al: Parkinsonian rigidity, dopa-induced dyskinesia and chorea—dynamic studies on the basal ganglia-thalamocortical motor circuit using PET scan and depth microrecording. **Acta Neurochir Suppl** 64:5–8, 1995
51. Holmes CJ, Hoge R, Collins L, et al: Enhancement of MR images using registration for signal averaging. **J Comput Assist Tomogr** 22:324–333, 1998
52. Ilinsky IA: Structural and connective diversity of the primate motor thalamus: experimental light and electron microscopic studies in the rhesus monkey. **Stereotact Funct Neurosurg** 54/55:114–124, 1990
53. Ilinsky IA, Kultas-Ilinsky K, Rosina A, et al: Quantitative evaluation of crossed and uncrossed projections from basal ganglia and cerebellum to the cat thalamus. **Neuroscience** 21:207–227, 1987
54. Jankovic J, Cardoso F, Grossman RG, et al: Outcome after stereotactic thalamotomy for parkinsonian, essential and other types of tremor. **Neurosurgery** 37:680–687, 1995
55. Jasper HH, Bertrand G: Thalamic units involved in somatic sensation and voluntary and involuntary movements in man, in Purpura DP, Yahr MD (eds): **The Thalamus**. New York: Columbia University Press, 1966, pp 365–390
56. Jones EG, Friedman DP, Hendry SHC: Thalamic basis of place and modality-specific columns in monkey somatosensory cortex: a correlative anatomical and physiological study. **J Neurophysiol** 48:545–568, 1982
57. Jones MW, Tasker RR: The relationship of documented destruction of specific cell types to complications and effectiveness in thalamotomy for tremor in Parkinson's disease. **Stereotact Funct Neurosurg** 54/55:207–211, 1990
58. Kall BA, Kelly PJ, Goerss S, et al: Methodology and clinical experience with computed tomography and a computer-resident stereotactic atlas. **Neurosurgery** 17:400–407, 1985
59. Laitinen L: Thalamic targets in the stereotaxic treatment of Parkinson's disease. **J Neurosurg** 24:82–85, 1966
60. Laitinen LV: Brain targets in surgery for Parkinson's disease. Results of a survey of neurosurgeons. **J Neurosurg** 62:349–351, 1985
61. Laitinen LV, Bergenheim AT, Hariz MI: Leksell's posteroventral pallidotomy in the treatment of Parkinson's disease. **J Neurosurg** 76:53–61, 1992
62. Lang AE, Lozano AM: Parkinson's disease. First of two parts. **N Engl J Med** 339:1044–1053, 1998
63. Lang AE, Lozano AM: Parkinson's disease. Second of two parts. **N Engl J Med** 339:1130–1143, 1998
64. Lenz FA, Kwan HC, Dostrovsky JO, et al: Single unit analysis of the human ventral thalamic nuclear group. Activity correlated with movement. **Brain** 113:1795–1821, 1990
65. Lenz FA, Kwan HC, Martin RL, et al: Single unit analysis of the human ventral thalamic nuclear group. Tremor-related activity in functionally identified cells. **Brain** 117:531–543, 1994
66. Lenz FA, Normand SL, Kwan HC, et al: Statistical prediction of the optimal site for thalamotomy in parkinsonian tremor. **Mov Disord** 10:318–328, 1995
67. Lenz FA, Tasker RR, Kwan HC, et al: Selection of the optimal lesion site for the relief of parkinsonian tremor on the basis of spectral analysis of neuronal firing patterns. **Appl Neurophysiol** 50:338–343, 1987
68. Lenz FA, Vitek JL, DeLong MR: Role of the thalamus in parkinsonian tremor: evidence from studies in patients and primate models. **Stereotact Funct Neurosurg** 60:94–103, 1993
69. Lim JY, De Salles AA: Sequential postoperative appearance of radiofrequency pallidotomy lesions on MRI. **Stereotact Funct Neurosurg** 69:46–53, 1997
70. Macchi G, Jones EG: Toward an agreement on terminology of nuclear and subnuclear divisions of the motor thalamus. **J Neurosurg** 86:670–685, 1997
71. Maendly R, Rugg DG, Wiesendanger M, et al: Thalamic relay for group I muscle afferents of forelimb nerves in the monkey. **J Neurophysiol** 46:901–917, 1981
72. Markham CH, Brown WJ, Rand RW: Stereotaxic lesions in Parkinson's disease: clinico-pathological correlations. **Arch Neurol** 15:480–497, 1966
73. Narabayashi H: Lessons from stereotaxic surgery using microelectrode techniques in understanding parkinsonism. **Mt Sinai J Med** 55:50–57, 1988
74. Narabayashi H: Physiological analysis of ventrolateral thalamotomy for rigidity and tremor. **Confin Neurol** 26:264–268, 1965
75. Narabayashi H, Yokochi F, Nakajima Y: Levodopa-induced dyskinesia and thalamotomy. **J Neurol Neurosurg Psychiatry** 47:831–839, 1984
76. Nowinski WL, Fang A, Nguyen BT, et al: Multiple brain atlas database and atlas-based neuroimaging system. **Comput Aided Surg** 2:42–66, 1997
77. Obrador S: A simplified neurosurgical technique for approaching and damaging the region of the globus pallidus in Parkinson's disease. **J Neurol Neurosurg Psychiatry** 20:47–49, 1957
78. Ohye C, Narabayashi H: Physiological study of presumed ventralis intermedialis neurons in the human thalamus. **J Neurosurg** 50:290–297, 1979
79. Ohye C, Saito U, Fukamachi A, et al: An analysis of the spontaneous rhythmic and non-rhythmic burst discharges in the human thalamus. **J Neurol Sci** 22:245–259, 1974
80. Ohye C, Shibasaki T, Hirai T, et al: Further physiological observations on the ventralis intermedialis neurons in the human thalamus. **J Neurophysiol** 61:488–500, 1989
81. Ohye C, Shibasaki T, Hirai T, et al: Tremor-mediating thalamic zone studied in humans and in monkeys. **Stereotact Funct Neurosurg** 60:136–145, 1993
82. Olivier A, Bertrand G: Stereotaxic device for percutaneous twist-drill insertion of depth electrodes and for brain biopsy. Technical note. **J Neurosurg** 56:307–308, 1982
83. Otsuki T, Jokura H, Takahashi K, et al: Stereotactic gamma-thalamotomy with a computerized brain atlas: technical case report. **Neurosurgery** 35:764–768, 1994
84. Page RD, Miles JB: Validation of CT targeting for functional stereotaxis with postoperative magnetic resonance imaging. **Br J Neurosurg** 8:461–467, 1994
85. Poggio GF, Mountcastle VB: The functional properties of ventrobasal thalamic neurons studied in unanesthetized monkeys. **J Neurophysiol** 26:775–806, 1963
86. Pollak P, Benabid AL, Limousin P, et al: Subthalamic nucleus stimulation alleviates akinesia and rigidity in Parkinsonian patients. **Adv Neurol** 69:591–594, 1996
87. Rouiller EM, Liang F, Babalian A, et al: Cerebellothalamocortical and pallidothalamocortical projections to the primary and supplementary motor cortical areas: a multiple tracing study in macaque monkeys. **J Comp Neurol** 345:185–213, 1994
88. Sakai ST, Inase M, Tanji J: Comparison of cerebellothalamic and pallidothalamic projections in the monkey (*Macaca fuscata*): a double anterograde labeling study. **J Comp Neurol** 368:215–228, 1996
89. Samuel M, Caputo E, Brooks DJ, et al: A study of medial pallidotomy for Parkinson's disease: clinical outcome, MRI location and complications. **Brain** 121:59–75, 1998
90. Schaltenbrand G, Bailey P: **Introduction to Stereotaxis, With an Atlas of the Human Brain**. Stuttgart: Thieme, 1959
91. Schaltenbrand G, Wahren P: **Atlas for Stereotaxy of the Human Brain, ed 2**. Stuttgart: Thieme, 1977
92. Seike M: A study of the area of distribution of the deep sensory neurons of the human ventral thalamus. **Stereotact Funct Neurosurg** 61:12–23, 1993

93. St-Jean P, Sadikot AF, Collins L, et al: Automated atlas integration interactive 3-dimensional visualization tools for planning and guidance in functional neurosurgery. **IEEE Trans Med Imaging** **17**:672–680, 1998
94. Starr PA, Vitek JL, Bakay RAE: Ablative surgery and deep brain stimulation for Parkinson's disease. **Neurosurgery** **43**: 989–1015, 1998
95. Stepniewska I, Preuss TM, Kaas JH: Thalamic connections of the primary motor cortex (M1) of owl monkeys. **J Comp Neurol** **349**:558–582, 1994
96. Sumanaweera TS, Glover GH, Hemler PF, et al: MR geometric distortion correction for improved frame-based stereotaxic target localization accuracy. **Magn Reson Med** **34**:106–113, 1995
97. Taren J, Guiot G, Derome P, et al: Hazards of stereotaxic thalamotomy. Added safety factor in corroborating x-ray target localization with neurophysiological methods. **J Neurosurg** **29**: 173–182, 1968
98. Tasker RR, Dostrovsky JO: What goes on in the motor thalamus? **Stereotact Funct Neurosurg** **60**:121–126, 1993
99. Tasker RR, Richardson P, Rewcastle B, et al: Anatomical correlation of detailed sensory mapping of the human thalamus. **Confin Neurol** **34**:184–196, 1972
100. Tasker RR, Siqueira J, Hawrylyshyn P, et al: What happened to VIM thalamotomy for Parkinson's disease? **Appl Neurophysiol** **46**:68–83, 1983
101. Tollefson TT, Burns J, Wilkinson S, et al: Comparative magnetic resonance image-based evaluation of thalamotomy and pallidotomy lesion volumes. **Stereotact Funct Neurosurg** **71**: 131–144, 1998
102. Tomlinson FH, Jack CR Jr, Kelly PJ: Sequential magnetic resonance imaging following stereotactic radiofrequency ventralis lateralis thalamotomy. **J Neurosurg** **74**:579–584, 1991
103. Vinas FC, Zamorano L, Dujovny M, et al: In vivo and in vitro study of the lesions produced with a computerized radiofrequency system. **Stereotact Funct Neurosurg** **58**:121–133, 1992
104. Zhang G, Guo Q, Wu S: CT analysis of postoperative changes after thalamotomy for Parkinson's disease. **Stereotact Funct Neurosurg** **64**:115–122, 1995

Manuscript received December 6, 2000.

Accepted in final form December 28, 2001.

Financial support for this project includes scholarships from The Parkinson Foundation of Canada (J.D.A.), Fonds de Chercheurs et l'Aide à la Recherche, Quebec (J.D.A.), Preston Robb Fellowship (J.D.A.), Fonds des Recherches Sante du Quebec (G.B.P. and D.L.C.), Medical Research Council of Canada (G.B.P., D.L.C., and A.F.S.) and operating grants from the Medical Research Council of Canada (G.B.P., A.F.S., and T.M.P.).

Address reprint requests to: Abbas F. Sadikot, M.D., Ph.D., Montreal Neurological Institute, 3801 University Avenue, Montreal, Quebec, H3A 2B4 Canada. email: sadikot@bic.mni.mcgill.ca.